

Linear systems approach to describing and classifying Fano resonances

I. Avrutsky,^{1,2} R. Gibson,^{1,3} J. Sears,³ G. Khitrova,³ H. M. Gibbs,³ and J. Hendrickson¹

¹*Sensors Directorate, Air Force Research Laboratory, Wright-Patterson Air Force Base, Ohio 45433, USA*

²*Department of Electrical and Computer Engineering, Wayne State University, 5050 Anthony Wayne Drive, Detroit, Michigan 48202, USA*

³*College of Optical Sciences, University of Arizona, 1630 E University Blvd., Tucson, Arizona 85721, USA*

(Received 24 July 2012; revised manuscript received 23 January 2013; published 13 March 2013)

We show that a generalized asymmetric resonant line shape derived elsewhere from rigorous electromagnetic calculations [Gallinet and Martin, *Phys. Rev. B* **83**, 235427 (2011)] and from the two-oscillators model [Joe *et al.*, *Phys. Scr.* **74**, 259 (2006)] can also be obtained using a very general assumption that the spectral dependence of the scattering amplitudes is given by the transfer function of a linear system. We reformulate the line shape equation and show that in the case of a first-order transfer function all possible line shapes can be presented by a weighted sum of the original Fano and Lorentzian line shapes. We propose a new two-parameter classification scheme for asymmetric resonances with one parameter δ being the asymmetry factor of the Fano component and the other parameter η quantifying the relative weight of the Fano and Lorentzian components of the line shape. The proposed formula is used to fit experimental spectra of a silicon photonic crystal cavity nanobeam interrogated using a fiber taper probe.

DOI: [10.1103/PhysRevB.87.125118](https://doi.org/10.1103/PhysRevB.87.125118)

PACS number(s): 42.25.Bs, 78.67.Pt

I. INTRODUCTION

Asymmetric spectral line shapes were first explained by Fano in studies of the absorption spectra of Rydberg atoms of noble gases¹ and in inelastic scattering of electrons by helium atoms.² It has been pointed out that in a system described by a Hamiltonian \hat{H} , coupling $V_{E'} = \langle \psi_{E'} | \hat{H} | \varphi \rangle$ of a discrete state $|\varphi\rangle$ with energy $E_\varphi = \langle \varphi | \hat{H} | \varphi \rangle$ to a continuum of states $|\psi_{E'}\rangle$ with energies E' in the range that includes E_φ , leads to the formation of a perturbed state

$$|\phi\rangle = |\varphi\rangle + p.v. \int \frac{V_{E'} |\psi_{E'}\rangle}{E_\varphi - E'} dE', \quad (1)$$

where *p.v.* indicates the principal value of the integral. Probability of transitions involving such states, normalized by the probability of transitions for nonperturbed states, is then given by the Fano formula

$$F(\varepsilon) = \frac{(q + \varepsilon)^2}{1 + \varepsilon^2}, \quad (2)$$

where q is the asymmetry factor and ε represents the scale of reduced energies such that the resonant transitions appear at $\varepsilon = 0$ and nonperturbed transitions have unit half-width.

The asymmetric Fano-like line shape appears in various physical systems described in terms of oscillations and waves,³ including scattering of particles in quantum mechanics,⁴ quantum transport phenomena,⁵ and electron-phonon coupling in superconductors.⁶ In photonics, the asymmetric line shape emerges when scattering (transmission, reflection, etc.) of a lightwave involves two channels, one of which is nonresonant broadband and the other mediated by a narrowband resonant excitation. Even if the Fano line shape may not be referred to explicitly, the scattering spectra reveals distinctive asymmetric features. Examples include waveguide gratings,^{7–10} photonic crystals,^{11–15} (nano)cavities,^{16,17} quantum confined structures,^{18,19} and resonant plasmonic structures.^{20–24}

These systems are usually complex enough that simulation of the scattering spectra must rely upon sophisticated

numerical calculations. The Fano resonances then appear as a result of heavy computations. Various analytical theories would then be developed to interpret the numerical simulations by identifying and quantifying the resonant and nonresonant scattering channels whose interference produces asymmetric spectral features.

Rigorous calculations such as in Ref. 23 revealed that the asymmetric resonant line shape may be given by a more general formula than the original Fano equation (2):

$$F(\varepsilon) = \frac{(q + \varepsilon)^2 + \gamma^2}{1 + \varepsilon^2}, \quad (3)$$

with an additional line shape parameter γ . Likewise, the exactly solvable two-oscillators model in Ref. 25, when considering only a narrow spectral interval around the resonant frequency and with some additional assumptions, can be reduced to (3).

In this paper we show that the line shape (3) can be obtained using a very general assumption that the scattering amplitudes are given by the transfer function of a first-order linear system. Despite all the differences between the studied structures, the asymmetric photonic resonances are strikingly similar in shape. As long as the derivation proposed here is general enough, it opens up the possibility for classification of asymmetric resonances that would be applicable to various physical systems. To accomplish this, we reformulate (3) into a weighted sum of the original Fano (2) and Lorentzian line shapes. The asymmetry parameter in the original Fano equation and the relative weight of Fano and Lorentzian components becomes the basis for a two-parameter classification scheme of asymmetric resonances.

II. RESONANT RESPONSE OF A FIRST-ORDER LINEAR SYSTEM

Leaving aside the specifics of a particular system, in the case of a narrow, isolated single resonance, all feasible line shapes can be easily found by considering light scattering as a

first-order linear process. In a narrow vicinity of the resonance, the distributed nature of the photonic system becomes less important and its response—the scattering amplitudes—is then given by a transfer function of a linear system. It is generally assumed (see, e.g., Ref. 26) that in the time domain (t) the response $f(t)$ of a linear system of order n to the input signal $g(t)$ is defined by a linear differential equation $Q^{(n)}(\hat{D})f(t) = P^{(n)}(\hat{D})g(t)$, where $\hat{D} = d/dt$ is the differential operator and $P^{(n)}(\hat{D})$ and $Q^{(n)}(\hat{D})$ are formal polynomials representing linear differential operators of order n . Then, in the frequency domain ω , the transfer function of the linear system is given by the ratio of polynomials $P^{(n)}(\omega)/Q^{(n)}(\omega)$. In particular, in the case of a single resonance ($n = 1$), the transfer function must be well approximated by a ratio of first-order polynomials $P^{(1)}(\omega)$ and $Q^{(1)}(\omega)$, so that

$$t(\omega) = \frac{P^{(1)}(\omega)}{Q^{(1)}(\omega)} = P \frac{\omega - \omega_z}{\omega - \omega_p}. \quad (4)$$

Here $t(\omega)$ is the scattering amplitude (say, amplitude transmission coefficient), ω is the radian frequency, $P = p \exp(i\phi)$ is the scattering amplitude far from the resonance, with p and ϕ being the magnitude and phase of P , $\omega_p = \omega_p^R - i\gamma_p$ and $\omega_z = \omega_z^R - i\gamma_z$ are the complex-valued pole and zero of the transfer function, with ω_p^R and γ_p referred to as the resonant frequency and damping rate. Choice of the negative sign in the expressions for ω_p and ω_z is due to the convention that a wave propagating along a wave vector \mathbf{k} oscillates as $\sim \exp[i(\mathbf{k}\mathbf{r} - \omega t)]$. The pole ω_p of the transfer function (4) with negative imaginary part $-i\gamma_p$ then corresponds to a decaying eigenmode $\sim \exp(-i\omega_p t) = \exp(-i\omega_p^R t) \exp(-\gamma_p t)$. In the most general case, we should assume no limitation on how large or small the real and imaginary parts of ω_p and ω_z may be.

As an illustration, consider a classical analogy to Fano resonances in Ref. 25. This exactly solvable model is based upon coupled harmonic oscillators driven by an external force. To mimic the resonant and nonresonant channels of Fano scattering, one of the oscillators is set to have a large damping rate (wide “nonresonant” channel), while the other one is nearly lossless (resonant channel). With each oscillator described by a second-order linear differential equation, the system response is given by a rational function with, generally speaking, fourth-order polynomials. However, in a narrow vicinity of the resonant frequency, one can present the transfer function in the form of (4) and trace how the system parameters define ω_p and ω_z .

Equation (4) can further be modified by placing the beginning of the frequency scale at ω_p^R and normalizing the frequency shift by γ_p , that is, by introducing the normalized frequency scale $\varepsilon = (\omega - \omega_p^R)/\gamma_p$. The scattering intensity spectrum is then found as the absolute value squared of the scattering amplitude $T(\varepsilon) = |t(\varepsilon)|^2$:

$$T(\varepsilon) = p^2 \frac{(\delta + \varepsilon)^2 + \gamma^2}{1 + \varepsilon^2}, \quad (5)$$

where $\delta = (\omega_p^R - \omega_z^R)/\gamma_p$ is the Fano asymmetry factor and $\gamma = \gamma_z/\gamma_p$ is another line shape factor. Equation (5) is essentially equivalent to (3) derived elsewhere,^{23,25} however, the analysis based on the linear systems approach clearly shows

the connection between the line shape parameters δ and γ on one hand and zeros and poles of the transfer function on the other hand.

Equation (5) turns into the original Fano formula (2) when $\gamma = 0$. The second line shape factor γ did not appear in the original Fano analysis due to the specifics of the considered problem. An expression equivalent to (5) may be obtained by extending the Fano formula (2) to include complex values of q : $T(\varepsilon) = p^2 |q + \varepsilon|^2 / (1 + \varepsilon^2)$. A complex asymmetry factor was linked to decoherence in quantum systems.²⁷ Also, the coupled oscillators model²⁵ yields complex q parameter in case of an oscillator with nonzero losses. It is worth noting that expression (5) here is derived from a very general assumption (4), and thus line shape (5) must be a property of all linear systems whose transfer function in the frequency range of interest could be reduced to a first-order expression with a single pole and single zero.

Significance of the second line shape factor γ , or, equivalently, complex values of q , is emphasized by the following: The ratio of scattering intensity at the resonance to that well beyond the resonance $T_{\varepsilon=0}/T_{\varepsilon \gg 1} = \delta^2 + \gamma^2$ depends on both δ and γ . In the original Fano treatment, the absolute value of the symmetry parameter δ (denoted as real quantity q) is a measure of the relative strength of the resonant scattering amplitude compared to the nonresonant [to be exact, the ratio of transition probabilities in Ref. 2 is $(\pi/2)q^2$]. With $\gamma \neq 0$, one should use $\sqrt{\delta^2 + \gamma^2}$ instead. This might be quite an essential correction, especially when $\gamma^2 \gg \delta^2$.

Another important observation is that with $\gamma \neq 0$, the scattering intensity (5) never turns into zero, as noted in Ref. 23. The asymmetric resonances in photonics are often seen to be like that, which justifies using the two-parameter (δ and γ) formula (5) instead of the original Fano formula (2) with real q , which yields zero intensity at $\varepsilon = -q$.

In many technical papers, to fit a line shape that does not go through zero, the original Fano formula (2) is modified. Besides a scaling factor F_0 , a constant shift A_0 is added (see, e.g., Ref. 11):

$$F(\varepsilon) = A_0 + F_0 \frac{(q + \varepsilon)^2}{1 + \varepsilon^2}. \quad (6)$$

A simple mathematical transformation such as vertical shift and scaling appears to have a significant effect upon the physical meaning of the fitting parameters. The model function (6) can be converted into a form equivalent to (5) with $p^2 = A_0 + F_0$, $\delta = qF_0/p^2$, $\gamma^2 = (q - \delta)(1 + \delta q)/q$, and thus it is equally suitable for fitting the experimental or numerically simulated data. However, physical sense of the constants becomes quite convoluted which may lead to some misinterpretation of fitting results. In particular, the q parameter in (6) can no longer be used as a measure of relative contribution of the resonant and nonresonant channels to the total scattering amplitude. Indeed, the nonresonant ($|\varepsilon| \gg 1$) intensity according to (6) is $A_0 + F_0$, and it can be changed independently of q . Because of no immediate physical sense, the factors A_0 and F_0 practically never appear in the analysis of data fitting and the fitting parameter q in (6), instead of the proper quantity $\sqrt{\delta^2 + \gamma^2} = \sqrt{(A_0 + F_0 q^2)/(A_0 + F_0)}$, might be misleadingly assumed to be a measure of how strong

the resonant component of the scattering is compared to the nonresonant.

III. TWO-PARAMETER CLASSIFICATION OF FIRST-ORDER ASYMMETRIC RESONANCES

For the sake of convenience of classifying the asymmetric line shapes, it is useful to introduce another unitless parameter $\eta = 1/(1 + \gamma^2)$ mapping the entire range of γ^2 values $0 \leq \gamma^2 < \infty$ into $0 \leq \eta \leq 1$ with the value of $\eta = 0$ corresponding to the limit $\gamma^2 \rightarrow \infty$ and $\eta = 1$ corresponding to $\gamma^2 = 0$. The line shape equation (5) then takes a convenient form of the weighted sum of Fano and Lorentz line shapes with weight factors η and $(1 - \eta)$, respectively,

$$T(\varepsilon) = A \left[\frac{\eta(\delta + \varepsilon)^2}{1 + \varepsilon^2} + \frac{1 - \eta}{1 + \varepsilon^2} \right], \quad (7)$$

and the overall magnitude factor $A = p^2/\eta = p^2(1 + \gamma^2)$. This generalized asymmetric line shape will be referred to as a weighted Fano-Lorentz line shape. To be specific, the term Fano line shape will be attributed to spectral features that are described by the original Fano formula (2), or, equivalently, (7) with $\eta = 1$, or (5) with $\gamma = 0$. Equation (7) allows for a convenient description of a line shape in terms such as pure (100%) Fano, pure (100%) Lorentz, or Fano-Lorentz mixed in a proportion of η to $(1 - \eta)$.

When fitting the experimental data, besides A , δ , and η , one still needs an explicit reference to the resonant frequency ω_p^R and damping rate γ_p :

$$T(\omega) = A \left[\frac{\eta(\omega - \omega_p^R + \delta\gamma_p)^2}{(\omega - \omega_p^R)^2 + \gamma_p^2} + \frac{(1 - \eta)\gamma_p^2}{(\omega - \omega_p^R)^2 + \gamma_p^2} \right]. \quad (8)$$

The asymmetry factor δ and the second line shape factor η quantitatively define the shape of the spectral features. The parameter η indicates relative weight of Fano and Lorentzian components in the first-order asymmetric line shape. The numerical fit with (8) is also an instrument to locate the resonant frequency ω_p^R , which, generally speaking, no longer coincides with spectral locations of either maximum or minimum of $T(\omega)$, and damping rate γ_p of the resonant excitation channel. The corresponding resonance quality factor then is $Q = \omega_p^R/2\gamma_p$.

In (7), the case of $\eta = 0$ corresponds to a pure Lorentzian peak and the case of $\eta = 1$ to a pure original Fano line shape. Note that the Fano line shape (2) is not normalized and may take on values (much) larger than unity. Instead, it is scaled in such a way that out-of-resonance values asymptotically approach unity. At sufficiently large values of $|\delta|$, the case of $\eta = 1$ allows for the highest possible asymmetry with $T(\varepsilon)$ vanishing at some frequency $\varepsilon = -\delta$ and reaching values as large as $(1 + \delta^2)$ at $\varepsilon = 1/\delta$. With $\delta = 0$, the Fano line shape degenerates into a symmetric dip. By adding the two terms in (7) one then gets $T(\varepsilon)|_{\delta=0} = A[\eta + (1 - 2\eta)/(1 + \varepsilon^2)]$, which may turn out to be a constant [$T(\varepsilon) = A/2$ when $\eta = 1/2$] with no resonant features visible at all, or it could look like a Lorentzian peak ($\eta < 1/2$) or a symmetric dip ($\eta > 1/2$) with a nonzero background. Note that with $\delta = 0$ and $\eta \approx 1/2$, when resonant features are barely visible (e.g., excitation of a low-loss ring resonator), the relative contribution of the

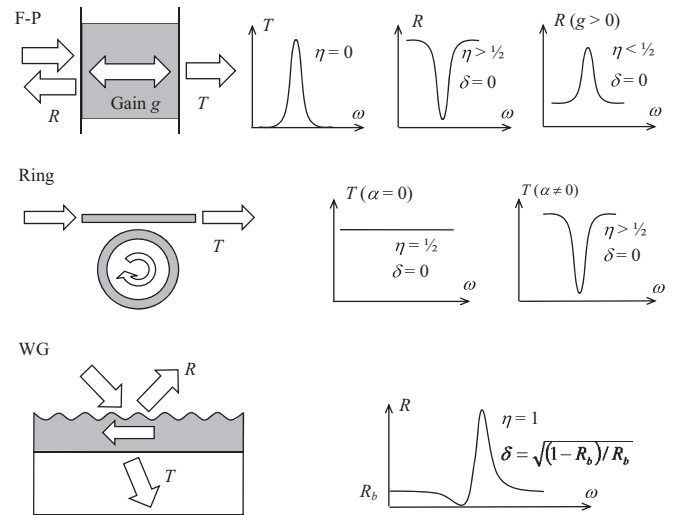


FIG. 1. Examples of photonic systems showing first-order resonances. From top to bottom: Fabry-Perot cavity (F-P), ring resonator (Ring), and waveguide grating (WG).

resonant channel compared to the nonresonant one is not close to zero as one might conclude using the fit (6) with $q = 0$. Instead, the right conclusion is that these channels provide about equal contribution: $\sqrt{\delta^2 + \gamma^2} = \sqrt{(1 - \eta)/\eta} \approx 1$. And indeed, sharp variation of the phase of the scattered (transmitted) wave at frequencies close to the resonance is an indication that the resonant channel certainly has a significant nonzero amplitude.

Some trivial examples of first-order line shapes are following (Fig. 1).

An isolated peak in the transmission spectrum of a Fabry-Perot resonator has close to zero background and, thus, its first-order approximation (7) becomes a Lorentzian peak ($\eta = 0$). The out-of-resonance reflection by a Fabry-Perot cavity is close to 100%, leaving no room for higher values; using the first-order linear systems approximation then requires $\delta = 0$. Though symmetric, this is one of the Fano line shapes (2). A reflection dip appears in (7) when $\eta > 1/2$, and it may reach zero if $\eta = 1$. It may also turn into a resonant reflection peak with some nonzero background ($\eta < 1/2$) if the medium inside the Fabry-Perot cavity provides optical amplification (but not lasing yet).

Flat intensity transmission response ($\delta = 0$, $\eta = 1/2$) is observed in a system with a channel waveguide coupled to a lossless ring cavity. Excitation of the cavity mode in this case leads to a pure phase response with transmission always kept at 100%. If the cavity has losses, a resonant dip appears ($\delta = 0$, $\eta > 1/2$).

Resonant reflection by a lossless waveguide grating reaches $R_{\max} = 100\%$ (anomalous reflection), while the out-of-resonance reflection is rather low (say, close to $R_b \sim 4\%$ for a glass-based waveguide). The line shape is not necessarily pure Fano (reflection does not necessarily go through zero in the vicinity of the resonance), but if it does, then $\eta = 1$ and δ is found from $1 + \delta^2 = R_{\max}/R_b = 1/R_b$, with positive (negative) δ corresponding to the reflection peak appearing at frequencies higher (lower) than the frequency of the reflection dip.

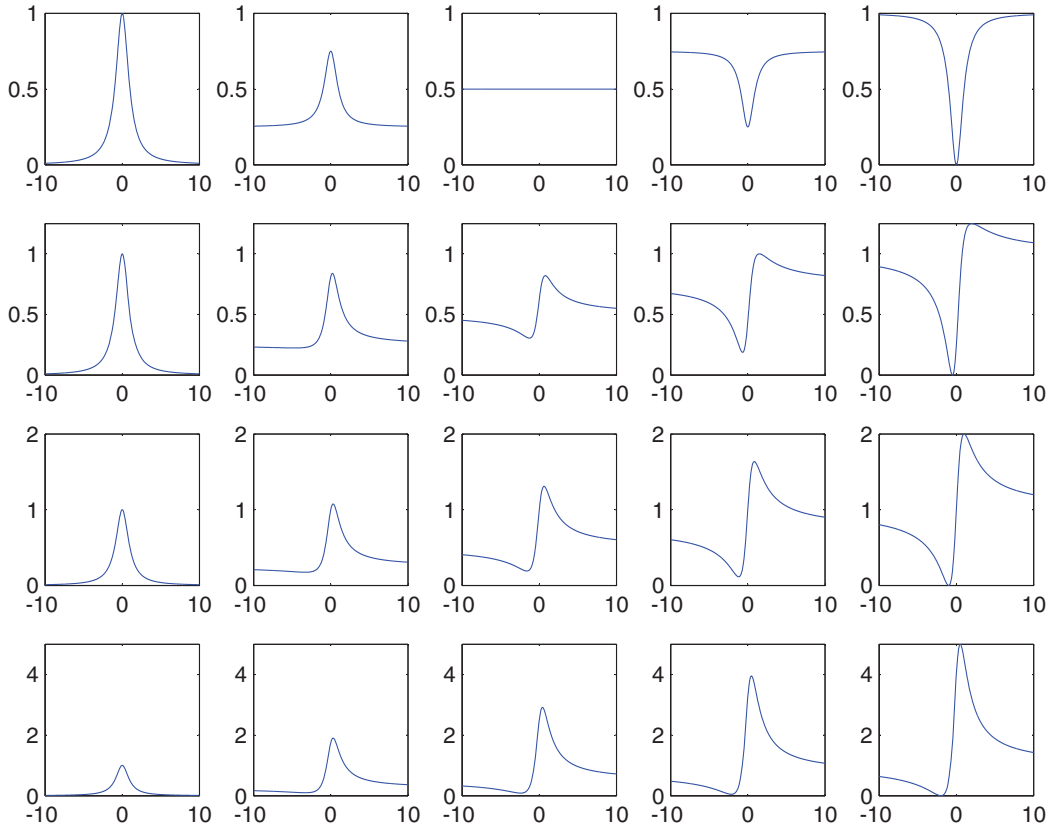


FIG. 2. (Color online) First-order resonant line shapes. Horizontal axis in all graphs shows normalized frequency ε . Vertical axis shows scattering intensity $T(\varepsilon)$ calculated according to (6) without normalization ($A = 1$). The graphs are arranged as follows: from left to right, $\eta = 0$ (Lorentz), $1/4$, $1/2$, $3/4$, 1 (Fano); from top to bottom, $\delta = 0$, $1/2$, 1 , 2 . Line shapes for negative values of δ can be obtained by flipping the axis of normalized frequency: $T(\varepsilon, \eta, -\delta) = T(-\varepsilon, \eta, \delta)$.

Representative line shapes calculated using (7) are shown in Fig. 2.

With $\eta = 0$ the line shape is Lorentzian regardless of δ . All the graphs in the first column are essentially identical. With $\eta = 1$ various Fano line shapes appear, starting from a symmetric dip at $\delta = 0$ at the top to highly asymmetric shapes with increasing δ . Note that the Fano line shapes always touch zero at some frequency ($\varepsilon = -\delta$). When the asymmetry factor is further increased so that $|\delta| \gg 1$ (not shown in Fig. 2), the asymmetry is preserved, but the zero-intensity frequency $\varepsilon = -\delta$ becomes shifted away from the resonance, while at frequencies close to the resonance the line shape resembles a Lorentzian. Generalized asymmetric line shape (7), except when $\eta = 1$, never goes to zero. Deviation of the scattering intensity from its out-of-resonance value may be quite small if $\eta \approx 1/2$ and $|\delta| \ll 1$.

Experimental observations and numerical simulations may lead to some other resonant line shapes substantially deviating from (7), such as in the case of the reflection spectrum of a Bragg grating. This essentially means that the single resonance (single zero, single pole) approximation neglecting the distributed nature of the photonic system is no longer valid. Other cases when (7) may not be quite accurate include systems with multiple overlapping resonances such that the rational function (4) with one zero and one pole no longer provides a good approximation for the transfer function.

However, the vast majority of practically important cases are perfectly described by the weighted Fano-Lorentz line shape (7) derived from a very general form of the rational function (4).

A particular nanocavity system that exhibits the resonance described by (7) is a 1D silicon photonic crystal cavity nanobeam, shown in the inset of Fig. 3, coupled to a fiber taper probe. Experimental details of such a system can be found in Refs. 28 and 29. Tuning the polarization of the light coupled to the nanobeam from the fiber taper changes the resonant line shape from a Fano-Lorentz line shape to pure Lorentzian line shape. Further work is in development that will describe this experimental system in more detail, show that it displays a variety of the line shapes shown in Fig. 1 with different input polarizations, and equate it to a simple solvable model. In Fig. 3 a Fano-Lorentz line shape (7) with $\eta = 0.506$ and $\delta = 0.055$, showing a nearly 50/50 contribution of a Fano line shape and a Lorentzian line shape, is fitted to the fiber transmission data for a particular polarization state. For the fit, A in (7) was taken to be a linear function of ω to take into account the slope of the data. As proposed above, these values would lead to a ratio between resonant and nonresonant scattering $\sqrt{\delta^2 + \gamma^2}$ of 0.99. Fitting with (6) the conventional scattering ratio parameter q is 0.84, leading to $\sim 18\%$ difference.

Work done in Ref. 30 shows simulations of plasmonic structures and their resonant modes. It is shown that the

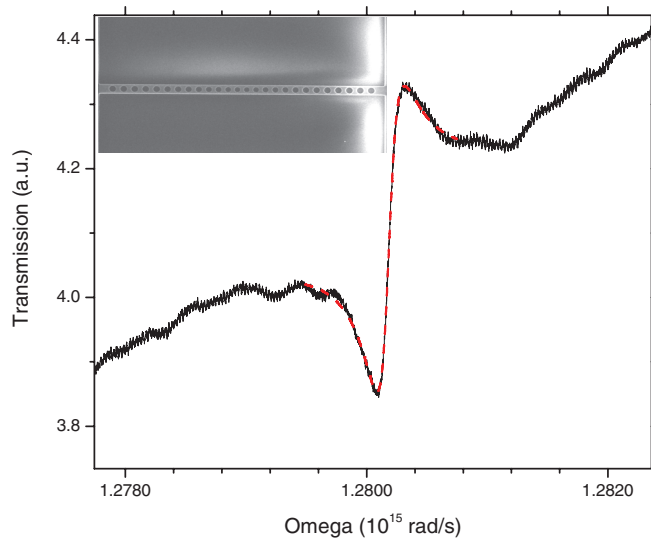


FIG. 3. (Color) Fiber taper transmission spectra of a 1D silicon photonic crystal nanobeam coupled to a fiber taper displaying a typical asymmetric line shape spectra (black) and a Fano-Lorentz fit (red). Inset: SEM of the photonic crystal cavity nanobeam. Length of the nanobeam is $10\ \mu\text{m}$.

resonant modes fit well to an equation from Ref. 22 which is equivalent to (7). If the standard Fano equation is used [Eq. (6)] the asymmetry terms in Table 1 of Ref. 30 would be significantly different. Another example of a system where the difference in asymmetry term is important comes about in Ref. 31 where a resonant mode of a plasmonic metamaterial is tuned to the vibrational mode of a biomolecule. Knowing the characteristics of the metamaterial and how those characteristics affect the asymmetry of the resonance can allow for better overlap between the resonant mode of

the plasmonic metamaterial and the vibrational mode of a biomolecule, leading to a stronger field enhancement. These two cases are examples where analyzing data with (7) instead of (6) proves to be beneficial.

IV. CONCLUSIONS

We have shown that asymmetric resonant line shapes derived elsewhere from rigorous electromagnetic calculations²³ and from the two-oscillators model²⁵ can also be obtained by treating the photonic resonance as a response of a first-order linear system. We have reformulated the line shape equation into a weighted sum of the Fano and Lorentzian line shapes and proposed a two-parameter classification scheme with one parameter being the asymmetry factor in the original Fano formula and the other one being the relative weight of the Fano and Lorentzian line shapes. The proposed line shape equation has been applied to the experimental spectra of one particular nanocavity system where the scattering ratios between resonant and nonresonant contributions are shown to be significantly different between the conventional Fano formula (6) and the Fano-Lorentz formula (7).

ACKNOWLEDGMENTS

I.A. acknowledges support by the Air Force Office of Scientific Research under the Summer Faculty Fellowship Program and by CPHOM, NSF Center for Photonics and Multiscale Nanomaterials, Material Research Science and Engineering Center Program DMR 1120923. J.H. would like to acknowledge support from the Air Force Office of Scientific Research (Program Manager Dr. Gernot Pomrenke) under Contract No. 12RY05COR. The Tucson group acknowledges support from Air Force Office of Scientific Research through Grant No. FA9550-10-1-0003 (Program Manager Dr. Gernot Pomrenke).

¹U. Fano, *Nuovo Cimento* **12**, 154 (1935).

²U. Fano, *Phys. Rev.* **124** 1866 (1961).

³A. E. Miroshnichenko, S. Flach, and Y. S. Kivshar, *Rev. Mod. Phys.* **82**, 2257 (2010).

⁴H. Feshbach, D. C. Peaslee, and V. F. Weisskopf, *Phys. Rev.* **71**, 145 (1947).

⁵E. Tekman and P. F. Bagwell, *Phys. Rev. B* **48**, 2553 (1993).

⁶E. T. Heyen, M. Cardona, J. Karpinski, E. Kaldis, and S. Rusiecki, *Phys. Rev. B* **43**, 12958 (1991).

⁷L. Mashev and E. Popov, *Opt. Commun.* **55**, 377 (1985).

⁸I. A. Avrutsky, A. S. Svakhin, and V. A. Sychugov, *J. Mod. Opt.* **36**, 1320 (1989).

⁹S. S. Wang, R. Magnusson, J. S. Bagby, and M. G. Moharam, *J. Opt. Soc. Am. A* **7**, 1470 (1990).

¹⁰E. Bonnet, X. Letartre, A. Cachard, A. V. Tishchenko, and O. Parriaux, *Opt. Quantum Electron.* **35**, 1025 (2003).

¹¹M. Galli, S. L. Portalupi, M. Belotti, L. C. Andreani, L. O'Faolin, and T. F. Krauss, *Appl. Phys. Lett.* **94**, 071101 (2009).

¹²S. Fan, *Appl. Phys. Lett.* **80**, 908 (2002).

¹³M. V. Rybin, A. B. Khanikaev, M. Inoue, A. K. Samusev, M. J. Steel, G. Yushin, and M. F. Liminov, *Photon. Nano.* **8**, 86 (2010).

¹⁴C. Grillet, D. Freeman, B. Luther-Davies, S. Madden, R. McPhe-dran, D. J. Moss, M. J. Steel, and B. J. Eggleton, *Opt. Express* **14**, 369 (2006).

¹⁵A. E. Miroshnichenko and Y. S. Kivshar, *Appl. Phys. Lett.* **95**, 121109 (2009).

¹⁶W. Liang, L. Yang, J. K. S. Poon, Y. Huang, K. J. Vahala, and A. Yariv, *Opt. Lett.* **31**, 510 (2006).

¹⁷B.-B. Li, Y.-F. Xiao, C.-L. Zou, Y.-C. Liu, X.-F. Jiang, Y.-L. Chen, Y. Li, and Q. Gong, *Appl. Phys. Lett.* **98**, 021116 (2011).

¹⁸M. Kroner, A. O. Govorov, S. Remi, B. Biedermann, S. Seidl, A. Badolato, P. M. Petroff, W. Zhang, R. Barbour, B. D. Gerardot, R. J. Warburton, and K. Karrai, *Nature (London)* **451**, 311 (2008).

¹⁹K. Kobayashi, H. Aikawa, A. Sano, S. Katsumoto, and Y. Iye, *Phys. Rev. B* **70**, 035319 (2004).

²⁰B. Luk'yanchuk, N. I. Zheludev, S. A. Maier, N. J. Halas, P. Norlander, H. Giessen, and C. T. Chong, *Nat. Mater.* **9**, 707 (2010).

- ²¹V. Giannini, Y. Francescato, H. Amrania, C. C. Phillips, and S. A. Maier, *Nano Lett.* **11**, 2835 (2011).
- ²²B. Gallinet and O. J. F. Martin, *Opt. Express* **19**, 22167 (2011).
- ²³B. Gallinet and O. J. F. Martin, *Phys. Rev. B* **83**, 235427 (2011).
- ²⁴S. H. Mousavi, A. B. Khanikaev, and G. Shvets, *Phys. Rev. B* **85**, 155429 (2012).
- ²⁵Y. S. Joe, A. M. Satanin, and C. S. Kim, *Phys. Scr.* **74**, 259 (2006).
- ²⁶B. P. Lathi, *Linear Systems and Signals*, 2nd ed. (Oxford University Press, Oxford, 2009).
- ²⁷A. Barnthaler, S. Rotter, F. Libisch, J. Burgdorfer, S. Gehler, U. Kuhl, and H.-J. Stockmann, *Phys. Rev. Lett.* **105**, 056801 (2010).
- ²⁸B. C. Richards, J. Hendrickson, J. D. Orlitzky, R. Gibson, M. Gehl, K. Kieu, U. K. Khankhoje, A. Homyk, A. Scherer, J.-Y. Kim, Y.-H. Lee, G. Khitrova, and H. M. Gibbs, *Opt. Express* **18**, 20558 (2010).
- ²⁹J. Hendrickson, A. Homyk, A. Scherer, T. Alasaarela, A. Säynätjoki, S. Honkanen, B. C. Richards, J.-Y. Kim, Y.-H. Lee, R. Gibson, M. Gehl, J. D. Orlitzky, S. Zandbergen, H. M. Gibbs, and G. Khitrova, *Quantum Optics With Semiconductor Nanostructures* (Woodhead Publishing, Cambridge, UK, 2012), Chap. 13.
- ³⁰B. Gallinet, O. J. F. Martin, *ACS Nano* **5**, 8999 (2011).
- ³¹C. Wu, A. B. Khanikaev, R. Adato, N. Arju, A. A. Yanik, H. Altug, and G. Shvets, *Nat. Mater.* **11**, 69 (2012).